Electromagnetics

A Deep Learning Method for Modeling the Magnetic Signature of Spacecraft Equipment using Multiple Magnetic Dipoles

Sotirios T. Spantideas[1], Anastasios E. Giannopoulos[1], Nikolaos C. Kapsalis[1] and Christos N. Capsalis[1]

[1] *National Technical University of Athens, School of Electrical and Computer Engineering, Athens, 15780, Greece*

Abstract — In the present work, a deep learning-based neural network for magnetic dipole modeling (MDMnet) is introduced in the framework of DC magnetic cleanliness for space missions. The developed method targets at modeling the static magnetic signature of a spacecraft unit that is obtained during the unit level characterization stage of the extensive pre-launch electromagnetic compatibility test campaign. By employing synthetic magnetic field data generated by virtual dipole sources, the MDMnet can be trained to accurately estimate the magnetic parameters of real equipment based on its near field measurements. The target of the proposed deep learning algorithm is, on the one hand, to effectively minimize the prediction errors (loss function) throughout the training process and, on the other hand, to enable the generalization of the model predictions, i.e. exhibit accurate model estimations with unseen magnetic field data. Extensive simulations towards the stabilization of the MDMnet hyperparameters are outlined, and indicative model inferences employing artificial magnetic field data are carried out. Finally, the MDMnet can achieve a predictive accuracy of 0.8 mm with respect to the dipole localization and 1% with respect to the magnetic field magnitude, verifying the potency of the developed method.

Index Terms — Electromagnetics, Deep Learning, Magnetic Dipole Modeling, Magnetic Cleanliness, Magnetic Signature,

I. INTRODUCTION

Conformance with stringent magnetic cleanliness requirements is a crucial concern in several space exploration missions that primarily focus on measuring the static magnetic fields originating from planetary and/or various objects. Such space missions include specialized instrumentation in order to capture the magnetic signature of these celestial bodies, namely high-resolution magnetic field sensors (typically tri-axial fluxgate magnetometers) [Glassmeier 2010]. The magnetometers that are mounted on the spacecraft, however, need to operate in zero-field conditions in order to provide accurate field measurements of the objects of interest. Therefore, the magnetic fields generated from the equipment inside the spacecraft or even the spacecraft enclosure itself need to be cautiously controlled and minimized [Mehlem 1978]. Static magnetic fields usually originate in the design and manufacturing of the spacecraft units, where materials with magnetic properties can be used, but their generation may be also attributed to the operation of actuation mechanisms (e.g. reaction wheels) and integral parts of the spacecraft (e.g. solar array) [ESA 2012].

Therefore, the magnetic cleanliness tests are a key pillar to accomplish the scientific objectives of various missions as part of the general electromagnetic compatibility and interference (EMC/EMI) campaign. Towards this direction, methods to meet the increasingly strict DC magnetic cleanliness requirements have been extensively studied, developed and implemented on many space programmes, such as BepiColombo, Juice and Solar Orbiter [Kaiser 2008, Brown 2019, Pudney 2019]. In the framework of all these programmes, magnetic measurements extend from unit level characterization (each spacecraft unit is individually subjected to measurements and modeling) to system level tests (measurement of the magnetic signature of the entire spacecraft).

The unit level characterization is the cornerstone of every magnetic cleanliness programme. This involves a standardized procedure targeting to capture the static near-field magnetic signature produced by an individual spacecraft unit and identifying a model consisting of virtual magnetic sources. Subsequently, the estimated models that are derived from all units can be employed to evaluate the total magnetic field and validate it against the system level measurements. According to [ESA 2012], several consequential actions are required, including magnetic budget simulations with regards to the placement of the units inside the spacecraft, investigation of design changes in their internal structures of each unit, higher-order demagnetization, etc.

The unit level near-field measurements are typically carried out in dedicated facilities, namely the Magnetic Coil Facility (MCF) and the Multi-Magnetometer Facility (MMF) [ESA 2012, Tsatalas 2019], using similar or identical measuring equipment with the onboard magnetic field sensors (fluxgate magnetometers). The sensors are placed in close proximity to the unit under test, while also aiming to effectively capture its spatial magnetic signature from various possible angles/orientations. Then, the acquired near-field magnetic data are modeled with well-established methods, the most prominent being the multiple dipole modeling (MDM) [Junge 2011]. The MDM method is principally based on the assumption that a set of virtual magnetic dipole sources can optimally reproduce the measured magnetic signature, thus accurately representing the original unit in terms of magnetic field generation. Notably, the implementation of the MDM method mainly relies on the determination of the model parameters, namely the position vectors of the magnetic dipoles inside the volume of the unit, as well as their magnetic moment vectors.

Multiple scientific space missions have taken advantage of the MDM method for their magnetic cleanliness programmes, for instance the Swarm mission, Solar Orbiter, Ulysses, etc. Towards applying the MDM method, both deterministic and stochastic optimization techniques are deployed; in particular, Genetic Algorithms (GAs) and Particle Swarm Optimization (PSO) are typical optimization methods used to identify the dipole parameters that accurately fit the measured magnetic field data [Carrubba 2012, Kapsalis 2012]. Importantly, these techniques exhibit adequate performance in terms of accuracy of the predicted field (deviation between the measured data and the magnetic field generated by the estimated model) and, additionally, demonstrate a satisfactory convergence speed for simple dipole sources. Nevertheless, since the determination of each dipole requires 6 model parameters (i.e. 3-D position and magnetic moment), the convergence time of these techniques becomes gradually elongated for increasing complexity of the magnetic sources comprising the unit, or the algorithms may even converge at suboptimal solutions [Spantideas 2016].

Driven by the ability of neural networks to efficiently estimate extremely complex functions, the present work introduces a deep learning algorithm for solving the MDM (MDMnet) inverse electromagnetic problem [Erricolo 2019]. The MDMnet is employed in order to learn (map) the relation between the input (magnetic field measurements) and the output (parameters of the dipole sources) via training with synthetic data. To obtain labeled data for the supervision of the model, simulated datasets containing multiple magnetic field data/model parameters pairs are generated and used to train the neural network. The training targets to adjust the MDMnet weights, so as to (i) minimize the defined loss function (mean square error between the actual dipole parameters and the predicted outputs of the model) and (ii) ensure generalization capabilities, i.e. achieve enhanced accuracy not only for the training samples, but also for data that have not been encountered by the algorithm during the training phase (in-sample and out-of-sample data). The main benefit of using a pre-trained network-based predictor is the ability to make inferences in near-real time and without considerable computational effort. In this context, the pre-trained model can be implemented directly on near-field measurement of real spacecraft equipment from the MCF or MMF facilities and provide predictive services in near-zero-time, even when complex scenarios are considered.

II. MATHEMATICAL FORMULATION

A. Background

According to the MDM method, the magnetic field generated by a unit under test is equal to the superposition of the fields produced by its magnetic dipoles, assuming that the unit contains $j = 1, 2, \dots, M$ dipoles. The magnetic flux density vector (herein referred as magnetic field) due to the presence of the j^{th} dipole source can be expressed [Mehlem 1978, Jackson 1999]:

$$\mathbf{B}_{ij} = \frac{\mu_0}{4\pi}\left[\frac{3\left(\mathbf{r'}_i - \mathbf{r}_j\right)\left[\left(\mathbf{r'}_i - \mathbf{r}_j\right)\cdot \mathbf{m}_j\right]}{\left|\mathbf{r'}_i - \mathbf{r}_j\right|^5} - \frac{\mathbf{m}_j}{\left|\mathbf{r'}_i - \mathbf{r}_j\right|^3}\right], \quad (1)$$

where $\mathbf{r'}_i = (x_{i_0}, y_{i_0}, z_{i_0})$ denotes the position of the i^{th} measurement point in Cartesian coordinates, $\mathbf{r}_j = (x_j, y_j, z_j)$ and $\mathbf{m}_j = (m_{x_j}, m_{y_j}, m_{z_j})$ stand for the position and magnetic moment vectors of the j^{th} dipole source inside the unit under test and μ_0 is the permeability of free space. The total magnetic field at the location of the i^{th} measurement point (magnetometer) can be calculated in components by summing up all the contributions from the M dipole sources:

$$\mathbf{B}_i = \sum_{j=1}^{M} B_{x_{ij}}\,\hat{\mathbf{x}} + \sum_{j=1}^{M} B_{y_{ij}}\,\hat{\mathbf{y}} + \sum_{j=1}^{M} B_{z_{ij}}\,\hat{\mathbf{z}} \quad (2)$$

B. Proposed Method

Without loss of generality, the geometrical shape of the unit under test is considered cuboid with dimensions $L \times W \times H$. Since the magnetic field sources can be located anywhere inside the volume of the unit, the position components of the training dipole parameters are generated according to the uniform distribution in the intervals $[-L/2, L/2]$, $[-W/2, W/2]$ and $[0, H]$ for the (x_j, y_j, z_j) components, respectively. Similarly, the values for the components of the magnetic moments $(m_{x_j}, m_{y_j}, m_{z_j})$ can also be drawn from a uniform distribution in the interval $[-m_{max}, m_{max}]$, where m_{max} is the maximum value of the magnetic moment. It is also worth noting that different distributions may be used to generate magnetic moment data, without having a significant impact on the results of the proposed method.

The generated values for the parameters of the dipoles are then employed in Eq. (1) (and Eq. (2) if more than one dipoles are considered for the model of the unit) in order to generate the magnetic field at $i = 1, 2, \dots, N$ measurement points and create multiple simulated measurements. Finally, these $p = 1, 2, \dots P$ pairs of magnetic field and dipole(s) parameters are used for the training of the neural network.

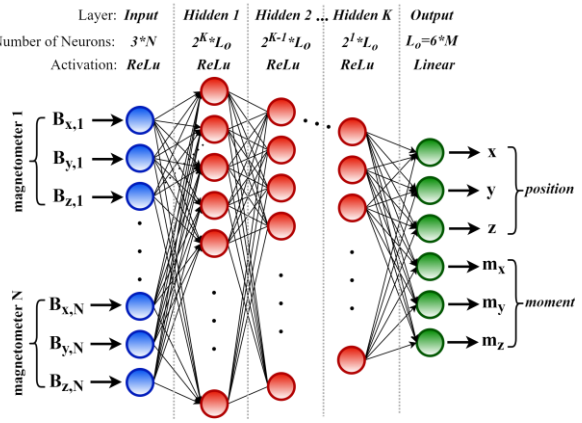

Fig. 1. Number of neurons and corresponding activation functions of input, output and hidden layers of the fully-connected MDMnet.

In this study, the MDMnet is deployed to solve a regression problem with supervised learning, targeting at learning the mapping function between the multi-site magnetic field measurements and the characteristics of the equivalent dipole. The dimensions of the neural

network (input, output and hidden layers) are depicted in Fig. 1. The input layer consists of $3 \times N$ neurons, since N tri-axial magnetic field sensors are considered for the measurement of the magnetic signature of the unit. Moreover, the output layer is $6 \times M$ neurons, considering that 6 parameters are used to describe each of the M magnetic dipoles. Finally, the number of neurons in the K hidden layers (intermediate layers between the input and output of the neural network that apply non-linear data transformation through an activation function [Goodfellow 2016]) are associated with the dimensions of the output layer, i.e. the number of dipole parameters to be estimated.

The P generated data pairs are used to train the neural network. The target is to adjust the weights of the neurons in order to minimize the loss function, i.e. the deviation between the actual positions and moments of the dipoles with respect to the output of the neural network (predicted values). We used an L2 loss function which can be expressed as:

$$F = \frac{1}{6 \cdot P \cdot M} \sum_{p=1}^{P} \sum_{j=1}^{M} \sum_{h=1}^{6} (Y_{hjp} - \hat{Y}_{hjp})^2 , \quad (3)$$

where $Y_{hj} = (x_j, y_j, z_j, m_{x_j}, m_{y_j}, m_{z_j})$ stands for the actual 6 parameters of the j^{th} magnetic dipole and $\hat{Y}_{hj}$ stands for the parameters estimated by the neural network. The algorithm performs multiple epochs (defined as the number of complete scans of the whole training dataset with multiple "feed-forward and back-propagation" cycles) during the training phase. In each epoch, the input and output values of all data pairs are used to update the neuron weights through the back propagation process [Goodfellow 2016]. The process converges when the objective function of Eq. (3) is substantially minimized, i.e. the weights of the neural network are properly adjusted to predict the output dipole parameters of all data samples.

III. SIMULATION RESULTS

A. Simulation Setup

In order to verify the proposed methodology, it is assumed that the unit level magnetic measurements are performed in the MMF facility, where 12 magnetic field sensors are used to simultaneously capture the signature of the unit [Tsatalas 2019], as depicted in Fig. 2.

The equally-spaced magnetometers are configured across 2 circles above and below the table in which the unit is placed at a radius of 25 cm and a height of ± 10 cm. Moreover, it is assumed that the unit's dimensions are $20 \times 20 \times 10$ cm^3 and its magnetic signature can be well represented by a single dipole source, having a maximum magnetic moment of ± 10 mAm^2 only in the z-direction.

Initially, $P = 10000$ data pairs are generated in order to evaluate the performance of the algorithm. Following the presented methodology, the MDMnet is configured with 36 neurons in input layer and 6 neurons in the output layer. Before the fine-tuning simulations, the number of hidden layers is varied from 1 to 9 and the learning rate ranges from 0.01 to 0.0001. The rectified linear (ReLu) activation function is adapted to the neurons of all layers, except for those of the output layer, to which the linear activation is employed. The MDMnet construction and the training/validation simulations were carried out in Python 3.8 and TensorFlow 2.3 (using the Adam optimizer).

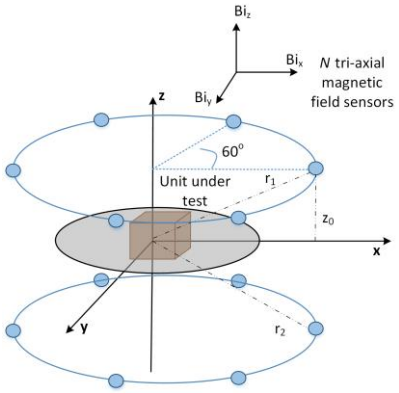

Fig. 2. Simulated measurements setup configuration using multiple magnetic field sensors (depicted as light blue circles) around a table that the unit under test is placed.

B. MDMnet Fine-Tuning

In order to determine the training hyper-parameters of the MDMnet, training/validation split of the data pairs P is set to 90%/10%. The selection criteria regarding the number of MDMnet hidden layers rely on three metrics that are extracted from the validation data. For each MDMnet configuration with varying number of hidden layers, the model is initially trained and then inferred employing 1000 validation scenarios. The calculation of the average position deviation between the actual dipole's parameters and the output of the MDMnet algorithm may be performed as follows:

$$\Delta r = \frac{1}{0.1 \cdot P} \sum_{p=900}^{P} \left[(x_p - \hat{x}_p)^2 + (y_p - \hat{y}_p)^2 + (z_p - \hat{z}_p)^2 \right] \quad (4)$$

and similarly regarding the average deviation of the magnetic moment.

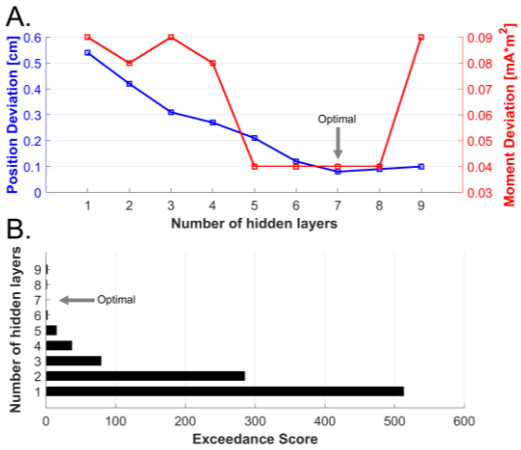

Fig. 3A. Deviation of position (in cm) and magnetic moment (in mAm^2) for varying number of hidden layers and 3B. Occurrences of position deviation greater than 0.5 cm (exceedance score) for different number of hidden layers.

This article has been accepted for publication in a future issue of this journal, but has not been fully edited. Content may change prior to final publication. Citation information: DOI 10.1109/LMAG.2021.3069374, IEEE Magnetics Letters

Furthermore, the exceedance score (i.e. number of validation scenarios that the position deviation is greater than a specific threshold) is also calculated. To ensure significant accuracy in the prediction of the dipole's position, the threshold is set at $\Delta r < 0.5$ cm [Tsatalas 2019]. Fig. 3 illustrates the position and moment deviation (panel A), as well as the exceedance score (panel B) as a function of the number of hidden layers. Evidently, the densification of the MDMnet is positively correlated with its performance, exhibiting locally optimal accuracy with the usage of 7 hidden layers.

Regarding the learning rate stabilization, similar simulations using 7 hidden layers and variable learning rates, i.e. {0.01, 0.001, 0.0001}, are conducted. As shown in Fig. 4, all learning rate configurations converge in semi-identical validation losses ($F < 0.001$), showing the optimal convergence speed in the scenario with a = 0.001.

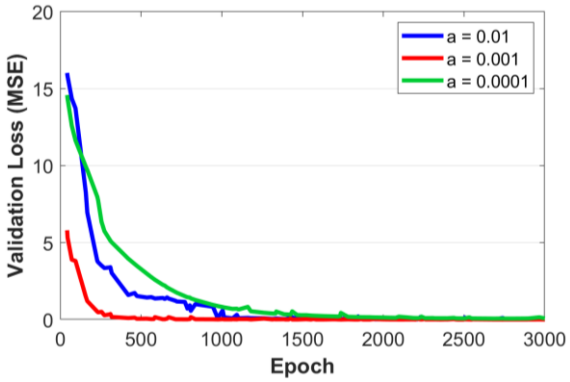

Fig. 4. Convergence of the validation loss function (MSE) with respect to the number of epochs for varying value of learning rate parameter a during the training session.

C. Verification Results

In order to evaluate the resulting estimations of the MDMnet (with 7 hidden layers and learning rate a=0.001) and verify its predictive performance with regard to the magnetic field signature, we exploit $P = 1000$ (out of training samples) different model predictions by using them for solving the forward problem. To this end, the magnetic field produced by the estimated models' parameters is calculated and compared to the input field of the neural network. This process guarantees that the estimated dipole from the MDMnet algorithm can accurately represent the magnetic signature of the virtual source.

In Fig. 5, the mean relative deviation (MRD) between the magnetic field magnitudes across all validation scenarios is depicted for all $i = 1, 2, \ldots 12$ observation points, along with the standard error (SE) bars of the mean. MRD extracted from measurement point i can be expressed by:

$$\mathrm{MRD}_i(\%) = 100\frac{1}{P}\cdot\sum_{p=1}^{P}\left(\frac{\sqrt{B_{x_{i,p}}^2 + B_{y_{i,p}}^2 + B_{z_{i,p}}^2} - \sqrt{B'^2_{x_{i,p}} + B'^2_{y_{i,p}} + B'^2_{z_{i,p}}}}{\sqrt{B_{x_{i,p}}^2 + B_{y_{i,p}}^2 + B_{z_{i,p}}^2}}\right), \quad (5)$$

where B and B' correspond to actual and predicted magnetic field values, respectively. Evidently, in all measurement points, the mean relative deviation (~1%) is within the range of 0.05 – 2%, indicating accurate reproduction of the magnetic field magnitude generated by the virtual dipole sources.

To precisely localize the MDMnet performance, Fig. 6 illustrates the mean absolute error (MAE ± SE) separately for each component of the magnetic signature between the predicted and actual field values (for the same 1000 scenarios). Evidently, MDMnet exhibits also adequate component-specific (~ 0.1 nT in x-, ~ 0.3 nT in y-, ~ 0.2 nT in z-component) predictive accuracy in all measurement points.

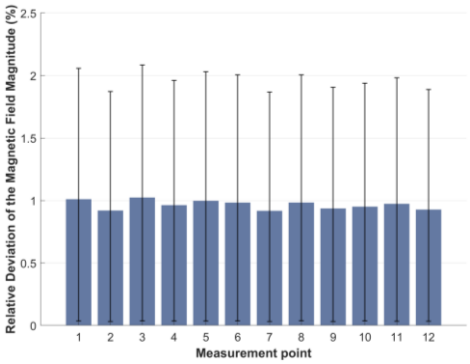

Fig. 5. Mean and Standard Error for the relative deviation (%) between actual and model-predicted magnitude of the magnetic field across the 12 measurement points.

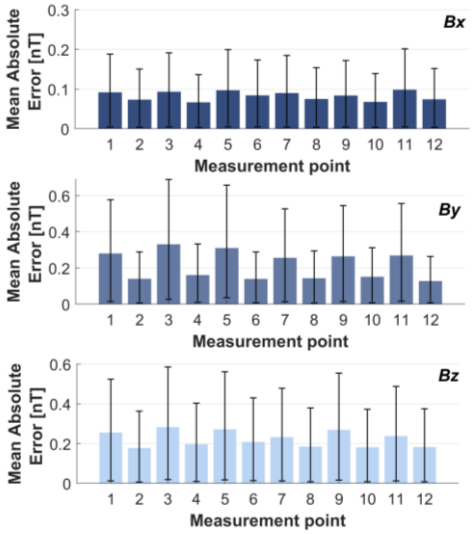

Fig. 6. Component-specific mean absolute error (in nT) between actual and model-predicted magnetic field across the 12 measurement points.

IV. CONCLUSION

In this work, a deep learning method for solving the MDM non-linear optimization problem is presented. A neural network (MDMnet) is trained with simulated data pairs of virtual sources/associated magnetic field. The pre-trained MDMnet is validated with different simulation scenarios in order to verify its potency. The resulting validation data confirm the MDMnet ability to accurately predict the magnetic source parameters.

The method may be further extended with multiple MDMnets, each one predicting a different number of virtual dipoles, introducing the concept of ensemble learning. Finally, another straightforward extension of the method involves the inclusion of measurements' setup configuration as inputs to the MDMnet.

REFERENCES

Glassmeier K H, Auster H U, Heyner D, Okrafka K, Carr C, Berghofer G, Anderson B J, Balogh A, Baumjohann W, Cargill P, Christensen U (2010), "The fluxgate magnetometer of the BepiColombo mercury planetary orbiter," *Planetary and Space Science*, *58*(1-2), pp.287-299, doi: 10.1016/j.pss.2008.06.018.

Mehlem K (1978), "Multiple magnetic dipole modeling and field prediction of satellites. *IEEE Transactions on Magnetics*, *14*(5), pp.1064-1071, doi: 10.1109/TMAG.1978.1059983.

ESA (2012), Space Engineering: Electromagnetic Compatibility Handbook, ECSS-E-HB-20-07A, Eur. Space Agency, ESA-ESTEC, Noordwijk, The Netherlands, http://everyspec.com/ESA/ECSS-E-HB-20-07A_47799/

Kaiser M L, Kucera T A, Davila J M, Cyr O S, Guhathakurta M, Christian E (2008), "The STEREO mission: an introduction," *Space Science Reviews*, *136*(1-4), pp.5-16, doi: 10.1007/s11214-007-9277-0.

Brown P, Auster U, Bergman J E S, Fredriksson J, Kasaba Y, Mansour M, Pollinger A, Baughen R, Berglund M, Hercik D, Misawa H (2019), "Meeting the magnetic EMC challenges for the in-situ field measurements on the Juice mission," *2019 ESA Workshop on Aerospace EMC (Aerospace EMC)*, pp. 1-6, IEEE, doi: 10.23919/AeroEMC.2019.8788942.

Pudney M, King S, Horbury T, Maksimovic M, Owen C J, Laget P (2019), "Solar orbiter strategies for EMC control and verification," *2019 ESA Workshop on Aerospace EMC (Aerospace EMC)*, pp. 1-6, IEEE, doi: 10.23919/AeroEMC.2019.8788930.

Tsatalas S, Vergos D, Spantideas S T, Kapsalis N C, Kakarakis S D, Livanos N A, Hammal S, Alifragkis E, Bougas A, Capsalis C N, Junge A (2019), "A novel multi-magnetometer facility for on-ground characterization of spacecraft equipment," *Measurement*, *146*, pp.948-960, doi: https://doi.org/10.1016/j.measurement.2019.07.016

Junge A, Marliani F (2011), "Prediction of DC magnetic fields for magnetic cleanliness on spacecraft," *IEEE International Symposium on Electromagnetic Compatibility (EMC)*, pp. 834–839, IEEE, doi: 10.1109/ISEMC.2011.6038424.

Carrubba E, Junge A, Marliani F, Monorchio A (2012), "Particle swarm optimization to solve multiple dipole modelling problems in space applications," *2012 ESA Workshop on Aerospace EMC*, pp. 1-6, IEEE.

Kapsalis N C, Kakarakis S D J, Capsalis C N (2012), "Prediction of multiple magnetic dipole model parameters from near field measurements employing stochastic algorithms," *Progress In Electromagnetics Research Letters*, 34, pp.111-122, doi: 10.2528/PIERL12030905.

Spantideas S T, Kapsalis N C, Kakarakis S D, Capsalis C N (2016), "A novel technique for accurate extrapolation of complex magnetic sources", *2016 ESA Workshop on Aerospace EMC (Aerospace EMC)*, pp. 1-5, IEEE.

Jackson J D (1999), *Classical Electrodynamics*, New York, John Wiley and Sons, pp. 184-188.

Goodfellow I, Bengio Y, Courville A, Bengio Y (2016), *Deep learning* (Vol. 1, No. 2). Cambridge: MIT press.

Erricolo D, Chen P Y, Rozhkova A, Torabi E, Bagci H, Shamim A, Zhang X (2019), "Machine learning in electromagnetics: A review and some perspectives for future research", *2019 International Conference on Electromagnetics in Advanced Applications (ICEAA)*, pp. 1377-1380, IEEE.

ANSWER TO REVIEWER 1

The authors of the manuscript "A Deep Learning Method for Modeling the Magnetic Signature of Spacecraft Equipment using Multiple Magnetic Dipoles" report on a deep learning algorithm to determine the magnetic dipole configuration from magnetic field measurements. The knowledge of the magnetic dipole configuration is critical for space probes, which study the magnetic signature for stellar objects. The existence of dipoles within the probe itself can contaminate the magnetic signature under investigation. The authors present an algorithm, which helps to solve the inverse problem, where the location and orientations of the dipoles is not known. The author test the algorithm with different parameters and validate the results.

We would like to thank Reviewer 1 for his/her comments and suggestions that helped us to clarify important issues and enhance the quality of the paper. Based on these comments/suggestions, several changes to the manuscript have been made.

The manuscript is well written but would benefit from the following revisions:

1) It is not clear, what "hidden layers" are.

The reviewer is correct. In order to clarify the definition of hidden layers, we have added the following phrase and the respective reference:

"(*intermediate layers between the input and output of the neural network that apply non-linear data transformation through an activation function [Goodfellow 2016]*)".

2) It appears that the parameter "a" in line 15 on page 4 was not defined. The reader can only guess that this is the learning rate.

We would like to thank the reviewer for his/her comment. This has been clarified in the updated version of the manuscript.

3) The authors refer to the magnetic field but use the unit Tesla and the variable B to quantify it. B is usually used for the magnetic induction and the unit for magnetic fields is A/m not Tesla, which is the unit of magnetic induction.

We would like to thank the reviewer for his/her comment. We actually calculate the magnetic induction (or magnetic flux density) **B** and refer to this as magnetic field. **B** has the units of Tesla, and taking into consideration that the relationship between **B** and **H** is linear ($\mathbf{B} = \mu_0\mathbf{H}$), Eq. (1) may be used to calculate the magnetic field **H** (in A/m), by simply omitting the constant μ_0. However, in order to be more concrete, we have clarified this issue before the definition of the magnetic induction (Eq. (1)).

4) The captions of the figures are generally not very clear and do not fully describe the figure.

As correctly suggested by the reviewer, the captions of the figures have been extended in order to clearly describe the respective figures.

5) In line 48 on page 3 it should read cm^3 not just cm

This has been corrected in the updated version of the manuscript.

6) The description within figure 2 is too small and hard to read.

As correctly suggested by the reviewer, the font size inside Fig. 2 has been increased for improved presentation purposes.

7) What is the difference between "in-sample" and "out-of-sample" data?

The reviewer's comment is valid. In principle, in-sample data are the training samples that are used for training purposes of the neural network, while out-of-sample data are data not previously encountered by the neural network and are used for validation of the deep learning algorithm. For clarification purposes, the following phrase has been added in the Introduction section:

"*(ii) ensure generalization capabilities, i.e. achieve enhanced accuracy not only for the training samples, but also for data that have not been encountered by the algorithm during the training phase (in-sample and out-of-sample data).*"

8) The authors state in the abstract that they can achieve an accuracy of 1% with respect to the magnetic field. Does this refer to the direction or magnitude of the magnetic field?

As correctly suggested by the reviewer, we have clarified in the Abstract that the accuracy of 1% corresponds to the magnitude of the magnetic field (also shown in the Verification Results subsection – Fig. 5). Regarding the direction of the magnetic field, we have also included in the results the mean absolute error (Fig. 6) for each individual component.

ANSWER TO REVIEWER 2

The manuscript is well written and the methods and results are reasonable. I do not have any objections to publish it in the present form.

We would like to thank Reviewer 2 for his/her feedback.